JOURNAL OF CATALYSIS 87, 86–92 (1984)

Modifications of the Atomic Structure of Platinum Aggregates Induced by H_2S, SO_2, and Elemental Sulfur Adsorption

G. BERGERET AND P. GALLEZOT[1]

Institut de Recherches sur la Catalyse, 2 Avenue Albert Einstein, 69626 Villeurbanne Cédex, France

Received June 14, 1983

The atomic structure of 1-nm Pt aggregates encaged in Y-type zeolites has been determined by radial electron distribution (RED) from X-ray diffraction data. The adsorption of H_2S on bare or H_2-covered aggregates produces a structure disorder and a rearrangement of atoms resulting in distorted (100) facets. The disorder is larger after adsorption of SO_2 and is complete upon adsorption of the ($H_2S + \frac{1}{2}SO_2$) mixture yielding elemental sulfur. The extent of disorder is probably related to the different sulfur coverages. The distortion of the (100) facets implies a preferential bonding of sulfur with only two of the four Pt atoms forming square facets. The relevance of these results to sulfur adsorption data on (100) Pt single crystal and to selective poisoning of catalytic reactions is discussed.

INTRODUCTION

The structures of adsorbed sulfur layers on metals have been studied extensively by surface science methods (*1, 2*). In most studies the top layer of metal is assumed to be a continuation of the bulk structure which implies that metal–sulfur bonding does not produce any atom displacement. However, ion scattering studies point to an outward expansion of the first metal layer (*3*). Metal atom displacement in the surface plane can also be expected when the coordination symmetry of the adatom is different from that of the adsorption site. Thus, sulfur atoms in a c(2 × 2) layer over Ni(100) are bonded to two nickel atoms although the adsorption sites have fourfold symmetry (*4*). However, because LEED is mainly sensitive to long range order, local displacement of atoms induced by strong adsorbates like sulfur can be overlooked.

Furthermore, the structures of small metal particles covered with sulfur are not well established. Theoretical calculations on Pt clusters predict that sulfur adsorption leads to a destabilization effect characterized by a decrease of the Pt–Pt bond strength (*5*). The mobility of the atoms is increased and restructuring is expected even at low temperature. The effect of H_2S adsorption on the structure of 1-nm Pt aggregates encaged in Y-type zeolite has been studied by radial electron distribution (RED) based on the Fourier transform of X-ray diffraction data (*6*). It was concluded that Pt–S bonding induces displacement of Pt atoms and results in a disordered structure. The total regeneration of the initial fcc structure was not completed even after H_2 treatment at 750 K.

In this work, the effect of H_2S adsorption was reinvestigated by RED on bare and H_2-covered 1-nm Pt aggregates. Radial distributions were also determined after SO_2 adsorption on H_2-covered aggregates and after adsorption of the stoichiometric mixture ($H_2S + \frac{1}{2}SO_2$) giving elemental sulfur (Claus reaction). This study was prompted by the findings of Maurel *et al.* (*7*) who introduced the concepts of selective poisoning and selective poisons, i.e., selective adsorption of sulfur on catalytic sites responsible for a particular type of catalytic reaction. Thus, H_2S and SO_2 were found to be nonselective, unlike elemental sulfur

[1] To whom correspondence should be addressed.

0021-9517/84 $3.00

which poisoned predominantly the sites responsible for hydrogenolysis. The aim of the present work was to study the effects of different modes of sulfur poisoning on the structure of Pt aggregates.

EXPERIMENTAL

Materials. The PtCeNa-Y zeolite was obtained from the NaY, Linde SK-40 sieve, by successive ion-exchanges, first, in water solutions of $Ce(NO_3)_3$ and second, in an ammonia solution of $PtCl_2$, as described previously (*8, 9*). The unit cell composition of the dehydrated zeolite, determined by chemical analysis of Pt, Ce and Na was $Pt_{11}Ce_1Na_{19}H_{12}Y$ ($Y = Al_{56}Si_{136}O_{384}$). One gram of zeolite was activated in flowing O_2 up to 600 K at 0.5 K min^{-1} and reduced at 540 K under 400 Torr (1 Torr = 133.3 Pa) of hydrogen pressure. Under these conditions, it has been shown that aggregates of 0.7–1.2 nm diameter nucleate in the supercage (*9*). It was confirmed by transmission electron microscopy on ultra-microtome cuts of the zeolite crystal that the aggregates in the present samples are within 0.9 ± 0.3 nm. They are denoted as 1-nm Pt aggregates as in previous articles.

Treatments. The reduced zeolite was evacuated at 700 K for 16 h under 10^{-5} Torr. Then, in a glove box flushed with oxygen-free dry argon, the zeolite was transferred into a stainless-steel cell equipped with a beryllium window designed to record the X-ray diffraction pattern under a controlled atmosphere. The zeolite powder was pressed into a rectangular cavity drilled at the back of the X-ray cell. The cell was connected to a vacuum and gas line to adsorb or to desorb gas at room temperature. Care was taken to introduce H_2S, SO_2, and ($H_2S + \frac{1}{2}SO_2$) in small increments to avoid any temperature increase due to the exothermic adsorption. Treatments at higher temperatures were performed in a quartz cell and then transferred into the X-ray cell in a glove box. The nomenclature and the treatments of the zeolite samples are given in Table 1.

TABLE 1

Treatments of the Platinum Zeolites

Sample	Treatments
Pt–I(H_2)	Zeolite activated at 600 K in O_2
	Reduced at 540 K in H_2 (400 Torr)
	Cooled under H_2, transferred in the X-ray cell, kept under H_2 during data recording
Pt–I(SO_2)	Previous sample (Pt–I(H_2)) evacuated at 300 K in the X-ray cell, 1 h
	Contacted with 10 Torr of SO_2 at 300 K, 10 min
	Evacuated at 300 K, kept under H_2
Pt–II(H_2)	Zeolite treated and kept as Pt–I(H_2)
Pt–II($H_2S + \frac{1}{2}SO_2$)	Pt–II(H_2) evacuated at 300 K contacted with 10 Torr of ($H_2S + \frac{1}{2}SO_2$) for 20 min at 300 K
	Evacuated at 300 K, kept under H_2
Pt–III(H_2S)	Previous sample (Pt–II($H_2S + \frac{1}{2}SO_2$) regenerated at 780 K under flowing H_2 for 6 h, kept under H_2
Pt–IV(H_2S)	Previous sample regenerated at 780 K under flowing H_2 for 26 h
	Evacuated at 780 K,
	Cooled to 300 K under vacuum,
	Contacted with 20 Torr of H_2S at 300 K
	Evacuated at 300 K, kept under H_2

RED analysis. X-Ray data collection and processing and calculation of the radial distribution function were performed as described previously (*10, 11*). The radial distribution function of a platinum-free NaHY zeolite was subtracted from those of the PtNaHY zeolites in order to eliminate the peaks corresponding to the atom pairs of the support.

RESULTS AND DISCUSSION

The radial distribution functions (rdf) of samples Pt-I(H_2), Pt-IV(H_2S), Pt-III (H_2S), Pt-I(SO_2), and Pt-II ($H_2S + \frac{1}{2}SO_2$) are given in Fig. 1, curves 1–5, respectively. The interatomic distances are given in Table 2. The adsorption of sulfur compounds on Pt aggregates produces two modifications of the rdf: (I) a decrease of the intensities of the Pt–Pt peaks due to a displacement disorder of the Pt atoms and (II) the appearance of new peaks indicating a specific rearrangement of Pt atoms. These features are discussed separately.

1. Sulfur-Induced Disorder

The rdf corresponding to 1-nm Pt aggregates covered with H_2(Pt-I(H_2), curve 1)

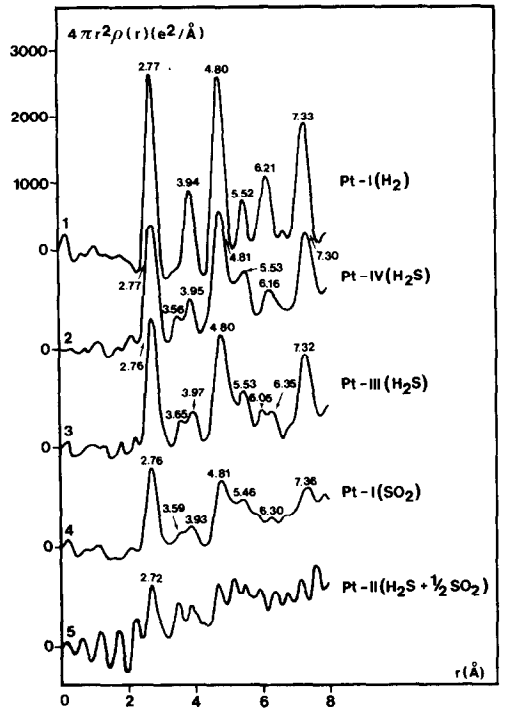

FIG. 1. Radial distribution functions of 1-nm Pt aggregates. (1) Aggregates covered by H_2, (2) adsorption of H_2S on bare aggregates, (3) adsorption of H_2S on H_2-covered aggregates, (4) adsorption of SO_2 on H_2-covered aggregates, (5) adsorption of ($H_2S + \frac{1}{2} SO_2$) on H_2-covered aggregates. Distance in Ångstroms (1 Å = 0.1 nm).

exhibits all the normal interatomic distances of bulk platinum as reported previously (*10, 12*). This has been attributed to dissociated hydrogen which completes the coordination of surface Pt atoms producing a relaxation of the contracted and distorted structure of bare aggregates.

The distributions corresponding to the adsorption of H_2S on the bare Pt aggregates (Pt-IV(H_2S), curve 2), and on the aggregates precovered with H_2 (Pt-III (H_2S), curve 3) are quite similar. In both cases the magnitudes of the three largest peaks (first, third, and seventh neighbors) are about 30% smaller than those of Pt–I(H_2) and the resolution is decreased due to peak broadening. Comparable modifications of the rdf of 1-nm Pt aggregate have been observed after CO adsorption (*12*) or dissociative hydrocarbon chemisorption (*13*). The decrease of peak heights was attributed to a displacement disorder of the Pt atoms due to the bonding with the adsorbates. The displacement disorder does not produce a large broadening of the peak because of the filtering by the Fourier transform used in the rdf calculation.

The adsorption of H_2S on the bare aggregates does not produce a larger disorder than on the H_2-covered aggregates and the interatomic distances are the same as in the reference sample (i.e., relaxed with respect to those of the bare aggregates). This means that in both samples a large fraction of the surface is covered by dissociated hydrogen which limits the extent of disorder. In Pt-IV (H_2S) the hydrogen atoms are generated by the dissociation of H_2S. The structural dis-

TABLE 2

Interatomic Distances

Sample	Interatomic distances (nm)						
	1st	2nd	3rd	4th	5th	6th	7th
Pt–I(H_2)	.277	.393	.480	.552	.621	.674	.733
Pt–IV(H_2S)	.277	.356–.395	.481	.553	.616[a]	[b]	.730
Pt–III(H_2S)	.276	.365–.397	.480	.553	.605–.635	[b]	.732
Pt–I(SO_2)	.276	.359–.393	.481	.546	[b]	[b]	.736
Pt–II(H_2S + $\frac{1}{2}SO_2$)	.272	[b]	[b]	[b]	[b]	[b]	[b]
Bulk Pt	.2774	.3923	.4805	.5548	.6203	.6795	.7339

[a] Broad.

[b] Unresolved or ill-resolved peak.

order induced by H_2S adsorption is less marked than that reported in a previous rdf study (*6*). In this early experiment, the temperature of adsorption could have been higher than 300 K because of the dissipation of the adsorption heat in a thick, compacted zeolite bed. Care has been taken in the present investigation to contact the zeolite progressively with gas increments.

The adsorption of SO_2 on the aggregates precovered with H_2 (Pt-I(SO_2), curve 4) produces severe modifications of the rdf. The three main peaks are 60% smaller than initially, indicating a larger displacement disorder of the Pt atoms than in the case of H_2S adsorption. SO_2 adsorption could lead to Pt–S and Pt–O bonding. The oxygen atom could either remain on the aggregate surface and contribute to the displacement disorder, as shown previously (*10, 12*), or more probably react with the H atoms initially present on the aggregate surface. Smaller hydrogen coverage may leave room for further SO_2 adsorption. Therefore in the case of SO_2 adsorption, the coverage by corrosive adsorbates like S and O is increased whereas the H_2 coverage which favors the presence of the ordered fcc structure is decreased. This accounts for a displacement disorder larger than that produced by H_2S adsorption.

The rdf corresponding to the adsorption of the (H_2S + $\frac{1}{2}SO_2$) mixture is given in Fig. 1. When the zeolite was contacted with 20 Torr of the mixture, the pressure gradually decreased down to 0.5 Torr after 20 min exposure. This is due to the Claus reaction ($2H_2S + SO_2 \rightarrow 3S + 2H_2O$) yielding elemental sulfur deposition in the zeolite pores and on the Pt aggregates. The absence of well-defined peaks on the rdf means that the final structure is almost completely disordered. The ripples observed in the rdf have no physical meaning. They are due to oscillations of the Fourier series probably resulting from a poor scaling of the X-ray intensities at large Bragg angles. This problem arises as a result of not taking into account the scattering of large amounts of sulfur. The structure disorder is much larger than in the case of H_2S or SO_2 adsorption. This can result from an increased sulfur coverage. However, the nature of the bonding between platinum and elemental sulfur produced by the Claus reaction could be different from that between platinum and sulfur produced by the dissociation of H_2S or SO_2. Unfortunately, it is not possible to check the first hypothesis because the amount of sulfur adsorbed on the Pt aggregate could not be evaluated with respect to that adsorbed on the support either by chemical analysis or by programmed thermodesorption under H_2 flow.

2. *Sulfur-Induced Rearrangement*

The rdf corresponding to H_2S adsorption (Pt-IV(H_2S), Pt-III (H_2S)) and to SO_2 adsorption (Pt-I(SO_2)) exhibits a splitting of the second peak initially at 0.393 nm. The fifth peak is also split or broadened to such an extent that it could correspond to two unresolved peaks. The presence of new peaks means that there is a new well-defined arrangement of Pt atoms which reproduces itself throughout the samples.

The second peak in the fcc structure corresponds to the diagonal of the square (100) facet. The splitting of the peak means that the C_{4v} symmetry of these sites lowers to C_{2v} symmetry. The first component of the doublet is located between 0.355 and 0.365 nm while the second appears at a slightly longer distance than the initial fcc peak. We suggest that the distortion of the fourfold symmetry site is induced by a preferential bonding of the adsorbed sulfur atom with only two of the four Pt atoms. This results in a shortening of the corresponding two distances and a slight lengthening of the other two (Fig. 2). Note that this arrangement must be reproducible from site to site in the same aggregate and in all the aggregates; otherwise the rdf would not give two separated peaks.

The rearrangement in the (100) facet does not affect the first and fourth distances nor the third and seventh distances which do

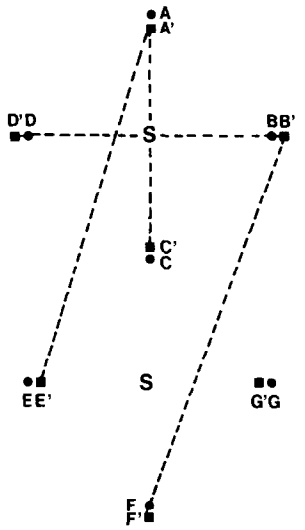

FIG. 2. Scheme of a seven-atom (100) facet. ●, Initial positions of the Pt atoms (regular 100) surface structure). ■, Positions of the Pt atoms after adsorption of two sulfur atoms bonded preferentially to A', C' and E', G', respectively. A'C' < AC = BD = 0.392 nm < B'D'; A'E' < AE = BF =0.620 nm < B'F'.

not belong to the (100) plane. On the other hand, the fifth peak initially at 0.620 nm is also split into two components. Figure 2 shows that the distortion of the (100) facet due to sulfur adsorption should result in the fifth peak becoming a doublet corresponding to distances smaller and larger, respectively, than 0.620 nm.

In a previous study (*6*) it was shown that the splitting of the second peak persists after hydrogen treatment at 750 K for 2 h while the other peaks, especially those occurring with a great multiplicity in the (111) plane (seventh peak), have recovered most of their initial intensity. This indicates that sulfur atoms coordinatively bonded to Pt atoms on distorted square facets are much more strongly bonded than sulfur atoms adsorbed on other sites and especially on (111) facets.

These results and interpretations given above are consistent with those derived from single crystal studies. Berthier *et al.* (*14*) have shown that on the Pt (100) face the sulfur atoms at saturation are arranged in a c(2×2) layer structure, each sulfur sitting at the center of the hollow square formed by four Pt atoms. The preferential bonding of sulfur by two metal atoms rather than by four equivalent atoms can be inferred from spectroscopic measurements (*15, 16*) and theoretical calculation (*17*). The C_{2v} bonding of sulfur on Ni(100) has been discussed by Fisher (*4*). No distortion of the underlying metal has been reported so far but it is questionable if LEED is sensitive enough to detect small local displacements of the metal atoms when long range order is preserved.

The stability of sulfur on the Pt(100) facets of the aggregate is in agreement with the larger heat of adsorption of sulfur on Pt(100) than on Pt(111) (*18*). Reconstruction and facetting occurring at high sulfur coverage on (100) faces are also indicative of a high stability of sulfur-covered (100) faces (*20*).

However, the analogy between aggregates and crystal faces cannot be extended too far. The surface structure of a single crystal is strongly dependent upon the ordered sublayers whereas there are almost no bulk atoms in 1-nm Pt aggregates. Therefore the structure flexibility in response to adsorbates is expected to be higher on the aggregates, in agreement with RED results (*10–13*).

3. *Atomic Structure and Catalytic Properties*

Sulfur poisoning of metal catalysts has been studied extensively (*1, 2, 19*); the comparison of literature data concerning the sulfur resistance and the regeneration of catalysts is difficult because different poisoning and regeneration treatments are used. The nature of the sulfur compound is seldom taken into account because at high temperatures the sulfur compounds are assumed to be hydrogenolysed into similar adsorbed species. This is not true at low temperature and even in the temperature range of saturated hydrocarbon conversion. Maurel *et al.* (*7*) have shown that re-

actions can be selectively poisoned according to the nature of the poison because of a selective adsorption of the sulfur compound on the sites catalyzing these reactions. The extent of sulfur coverage should also play a determining role.

The present work supports these views insofar as it demonstrates that the atomic structure of the Pt aggregates depends strongly upon the mode of sulfur introduction on the catalyst. The relation between catalytic properties and aggregate structure cannot be established yet because there are too many parameters involved. However, both the structure disorder and the rearrangement in (100) facets have obvious implications for the catalytic properties.

Structure disorder is due primarily to the extent of sulfur coverage increasing in the series $H_2S < SO_2 < S$. Different sulfur coverage should also result in different poisoning effects. The nature of the interaction between platinum and elemental sulfur could also be different from that of sulfur produced by H_2S dissociation.

The preferential bonding of sulfur with two Pt atoms on distorted (100) facets and the difficulty of eliminating sulfur from these sites means that the atoms in (100) facets are poisoned more strongly than the atoms in other facets. Therefore selective poisoning of a structure-sensitive reaction could possibly occur because the different sites are not poisoned in the same way.

CONCLUSION

This study shows that the atomic structure of 1-nm Pt aggregates is deeply modified by the adsorption of sulfur compounds. Pt–S bonding induces a displacement disorder of Pt atoms and a rearrangement in the (100) facets due to the preferential bonding of sulfur with two Pt atoms.

The modification of the aggregate structure depends upon the nature of the sulfur compound. Poisoning with H_2S results in a limited disorder whereas SO_2 and elemental sulfur have more deleterious effects on the structure. The extent of sulfur coverage is probably the major factor responsible for these differences. However, the coordination and binding energy of sulfur could change with the nature of the sulfur compound. Unfortunately, most of the literature data on metal/sulfur interactions have been obtained from H_2S adsorption experiments.

These results have obvious implications for catalysis. Since the sulfur compounds do not produce the same effect on the structure of the metal aggregate, they may conceivably act as selective poisons of structure-sensitive reactions. The stronger Pt–S bondings in (100) facets leading to a stable poisoning of the corresponding sites could also promote selective poisoning. Further studies should aim at determining possible changes of aggregate morphology occurring after poisoning and regeneration experiments. Indeed, reconstruction of the aggregate surface could be another factor influencing catalytic properties.

REFERENCES

1. Oudar, J., *Catal. Rev.-Sci. Eng.* **22,** 171 (1980).
2. Bartholomew, C. H., Agrawal, P. K., and Katzer, J. R., "Advances in Catalysis," Vol. 31, p. 135. Academic Press, New York, 1982.
3. Van Der Veen, J.F., Tromp, R. M., Smeenk, R. G., and Saris, F. W., *Surf. Sci.* **82,** 468 (1979).
4. Fisher, G. B., *Surf. Sci.* **62,** 31 (1977).
5. Halachev, T. D., and Ruckenstein, E., *Surf. Sci.* **108,** 292 (1981).
6. Gallezot, P., *in* "Proceedings, 5th International Conference on Zeolites, Naples 1980" (L. V. C. Rees, Ed.), p. 364. Heyden, London, 1980.
7. Maurel, R., Leclercq, G., and Barbier, J., *J. Catal.* **37,** 324 (1975).
8. Tri, T. M., Massardier, J., Gallezot, P., and Imelik, B., "Proceedings, 7th International Congress on Catalysis, Tokyo, 1980," p. 266. Elsevier, Amsterdam, 1981.
9. Gallezot, P., *Catal. Rev.-Sci. Eng.* **20,** 121 (1979).
10. Gallezot, P., Bienenstock, A., and Boudart, M., *Nouv. J. Chim.* **2,** 263 (1978).
11. Gallezot, P., and Bergeret, G., *J. Catal.* **72,** 294 (1981).
12. Gallezot, P., *Zeolites* **2,** 103 (1982).
13. Gallezot, P., *J. Chim. Phys.* **78,** 881 (1981).

14. Berthier, Y., Perdereau, M., and Oudar, J., *Surf. Sci.* **36,** 225 (1973).
15. Hagstrum, H. D., and Becker, G. E., *J. Vac. Sci. Technol.* **14,** 369 (1977).
16. Hagstrum, H. D., and Becker, G. E., *Proc. Roy. Soc. London Ser. A* **331,** 395 (1972).
17. Niemczyk, S. J., *J. Vac. Sci. Technol.* **13,** 364 (1976).
18. Bénard, J., Oudar, J., Barbouth, N., Margot, E., and Berthier, Y., *Surf. Sci.* **88,** L35 (1979).
19. Barbier, J., *in* "Metal-Support and Metal-Additive Effects in Catalysis" (B. Imelik *et al.*, Ed.), pp. 293. Elsevier, Amsterdam, 1982.
20. Schmidt, L. D., and Luss, D., *J. Catal.* **22,** 269 (1971).